Magnetic-resonance investigation of the ordering in randomly-site-diluted antiferromagnets: $KMnF_3$:Mg

G. D'Ariano
Istituto di Fisica dell'Università e Gruppo Nazionale di Struttura della Materia del Consiglio Nazionale delle Ricerche, 27100 Pavia, Italy

F. Borsa
Istituto di Fisica dell'Università e Gruppo Nazionale di Struttura della Materia del Consiglio Nazionale delle Ricerche, 27100 Pavia, Italy and Department of Physics and Ames Laboratory, Iowa State University, Ames, Iowa 50011

(Received 5 February 1982)

Measurements of ^{19}F NMR in a series of polycrystalline mixed paramagnetic compounds $KMn_xMg_{1-x}F_3$ with x varying over the whole concentration range have been performed as a function of temperature. The paramagnetic shift and the linewidth and relaxation time of the three NMR lines corresponding to those distinct classes of ^{19}F nuclei that have different numbers of nearest-neighbor magnetic ions were measured as the temperature approaches the transition temperature. The paramagnetic shifts of fluorine nuclei having one and two nearest-neighbor Mn ions compare well with the predictions of a simple random-molecular-field approximation (RMFA). It is shown that the substitution of Mn with Mg modifies locally the nuclear-electron transferred hfs interaction by about 20%. The linewidth of the two lines increases drastically as T_N is approached. The attempt to explain the data by utilizing Moriya's theory rescaled in the RMFA framework fails completely, indicating that the dynamic effects should be treated in real space. The antiferromagnetic ordering was monitored by measuring the rf susceptibility in zero external magnetic field. It is found that the antiferromagnetic transition is broadened by the concentration gradients present in the samples. The average transition temperature was determined as a function of the average concentration, and the results are compared with the theoretical predictions of recent calculations. Good agreement is found if one takes into account the concentration dependence of the exchange coupling constant.

I. INTRODUCTION

The investigation of a randomly diluted model magnetic system can be interesting from several points of view. The dependence of the ordering temperature and of the magnetic properties over the entire range of concentration x $(0<x<1)$ of magnetic atoms is related to the percolation theory. In particular, the collective-spin dynamics should be strongly affected by the reduction of the effective spatial dimensionality of the infinitely connected cluster with increasing magnetic dilution. Furthermore, there are a number of renormalization-group calculations which make predictions about the critical behavior of randomly disordered systems. Also, the fundamental question of whether or not a sharp phase transition can occur in a homogeneously random system is as yet unanswered.

Among the best magnetically diluted model systems is $KMn_xMg_{1-x}F_3$. $KMnF_3$ is a cubic perovskite crystal (a small tetragonal distortion takes place at $T_c \simeq 180$ K) with antiferromagnetic superexchange between nearest-neighbor (NN) Mn spins on a cubic sublattice mediated by a F^- ion at the midpoint of each cube edge. The anisotropy being very small, the system behaves as an almost ideal Heisenberg antiferromagnet. Nonmagnetic Mg^{2+} ions, isomorphous to Mn^{2+}, can be used to obtain a magnetically diluted crystal in which x-ray spectra show no change in lattice structure and no sign of clustering of Mg atoms.

The ^{19}F NMR in $KMn_xMg_{1-x}F_3$ has some interesting features arising from the location of the fluorine at midpoint between two Mn^{2+} ions, each of which strongly interacts with the ^{19}F nucleus by an isotropic transferred hyperfine coupling $A\vec{I}\cdot(\vec{S}_1+\vec{S}_2)$. In the paramagnetic phase, the ^{19}F NMR is shifted[1] by an amount proportional to $A(\langle S_{1z}\rangle+\langle S_{2z}\rangle)$ where z is the direction of the static magnetic field. In the diluted crystals three

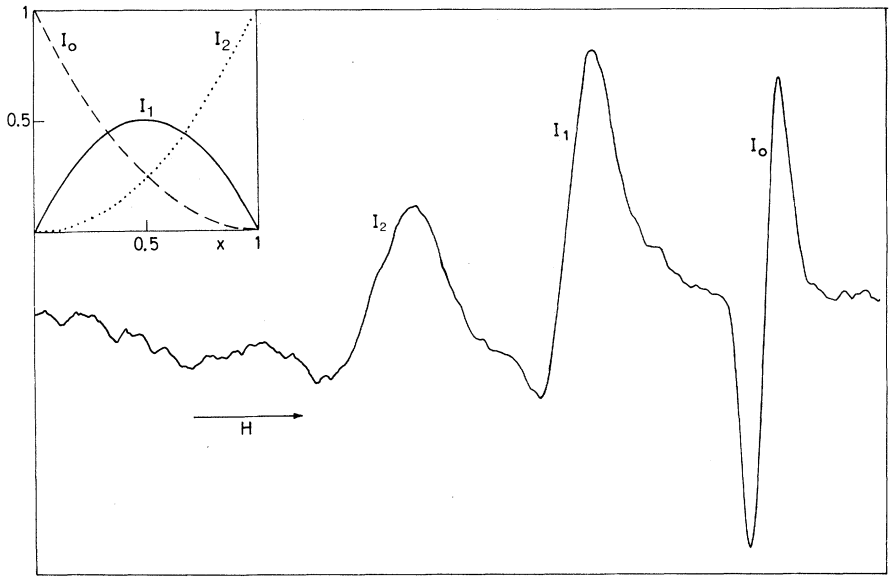

FIG. 1. Typical ^{19}F derivative NMR spectrum in a $KMn_xMg_{1-x}F_3$ sample with $x=0.78$. The recording was obtained at room temperature and at a resonance frequency of 22 MHz and the three resonances correspond to fluorine nuclei with different magnetic environment as explained in the text. In the upper left-hand corner the behavior of the relative intensities of the three lines as a function of Mn concentration for an ideal perfectly random solid solution is shown.

distinct ^{19}F nuclear-resonance lines are observed[2] corresponding to fluorines missing two, one, or zero manganese NN and their accompanying hyperfine fields. A typical NMR spectrum is shown in Fig. 1. The three lines are identified as I_0, I_1, and I_2 according to the number of Mn^{2+} NN to a given ^{19}F nucleus: I_0 (no NN), I_1 (one NN), and I_2 (two NN), with paramagnetic shifts of approximately 0, 1, and 2%, respectively.

The investigation of the nuclear-spin lattice relaxation of the fluorine I_0 has indicated[2] that this type of fluorine relaxes at sufficient magnetic dilution mainly by the interaction with the fluctuating dipolar fields due to Mn spins which are exchange isolated from their neighbors. On the other hand, the relaxation of fluorine of the type I_1 and I_2 is related to the decay of the autocorrelation and pair correlation functions, respectively, of Mn spins belonging to the infinitely connected cluster. Furthermore, the paramagnetic shift and the inhomogeneous broadening of the different NMR lines can yield information about the local electronic magnetization.

In this paper we present an investigation of the temperature dependence of the different parameters characterizing the ^{19}F NMR with the aim of exploring the building up of dynamic correlation and local magnetization both in the infinitely connected cluster and in the isolated Mn^{2+} clusters.

In Sec. II we give the details of the experimental methods while in Sec. III the NMR results for the different fluorine resonances are presented. The temperature dependence of the NMR parameters is discussed in Sec. IV mainly in terms of the random-molecular-field approximation (RMFA) for both the static and dynamic collective behavior of the disordered Mn^{2+} spin system. The dependence of the Néel temperature on the Mn^{2+} concentration was determined from radio frequency susceptibility measurements in zero external magnetic field and the results are also discussed in Sec. IV.

II. EXPERIMENTAL METHODS

The ^{19}F NMR experiments were performed by using both continuous wave (cw) techniques and pulsed NMR techniques. The cw measurements were performed with a modified Varian spectrometer operating at frequencies up to 60 MHz and by using a 1024 channels analyzer to perform the continous averaging. The pulse measurements were performed on a Bruker spectrometer operating at 22 MHz. The temperature was varied by a standard gas flow system using either nitrogen or helium as coolants and it was monitored by means of a Cu-Cn or Au(Fe)-Cn thermocouple. The temperature stability and gradients were typically within ± 0.5 °C.

Since the samples utilized in this work are polycrystalline, the NMR lines are broadened by the combination of demagnetization effects and of the

anisotropic dipolar interaction of the ^{19}F nuclei with the average electronic moment of the Mn^{2+} ions. The resulting line shape is asymmetric and field dependent (see Fig. 1). In order to obtain the homogeneous zero-field extrapolated linewidth, the following procedure was utilized for both lines I_1 and I_2. The width of the signal between the two closest points of maximum derivative was measured at room temperature for each sample at several external magnetic fields ranging from 2 to 10 KG. The data so obtained could be fitted to the linear relationship

$$\Delta H = \delta(T) + AK(T)H \quad (1)$$

where ΔH is the linewidth in the field H, $K(T)$ is the measured paramagnetic shift of the center of mass of the line, A is a fitting constant which includes the temperature-independent interaction parameters, and δ is the zero-field extrapolated linewidth. As the temperature was varied, only measurements at one or two values of the external field were performed and the value of δ was determined by using expression (1) together with the new measured value of the temperature-dependent shift K.

The samples were prepared at the University of California at Santa Barbara and are identical to the one used in the preliminary investigation.[2] The samples were analyzed by x ray at the Institute of Crystallography of the University of Pavia in order to verify the homogeneity and to determine the average concentration. The powder spectra do not reveal any sign of other phases nor of ordering or clustering of the isomorphous cations. Since the lattice constant a is known to vary linearly between the values for pure $KMnF_3$ and pure $KMgF_3$ we used the relation $x = a\,4.815 - 19.457$ to determine the concentration x from the measured value of a. The average concentrations of the samples used in this work are $x = 0.89$, 0.78, 0.74, 0.60, 0.52, 0.41, 0.305, and 0.19. It should be noted that the concentrations used in this work are the real average concentrations while the one used in the previous work[2] are the nominal ones, the difference being at most 0.04.

The radio frequency (rf) susceptibility was measured by using the same Varian spectrometer used for the NMR measurements tuned at 22 MHz. The rf probe containing the sample was placed in the center of a pair of Helmotz coils that allowed the application of a dc field which could be swept linearly between ± 300 G. By superimposing a small modulation (~ 0.5 G) at 80 Hz we could detect a signal both in the absorption and in the dispersion mode which is maximum around $H \sim 0$ and has a width of about 60 G. We identify the signal as an EPR signal of the Mn^{2+} ions. In fact at the operating rf frequency of 22 MHz the resonance Larmor field is only 7 G while the dipolar width is of the order of 60 G.

III. ^{19}F NMR RESULTS

In this section we present the experimental results by considering separately the data obtained on the three types of resonances I_0, I_1, I_2.

A. I_0 resonance: Fluorine nuclei with no Mn NN.

The measurements of spin-lattice relaxation rate as a function of concentration at room temperature have been discussed previously.[2–4] The emphasis here will be on new measurements of T_1 as a function of temperature.

1. Linewidth and signal intensity

The I_0 resonance has no measurable shift with respect to the ^{19}F resonance in $KMgF_3$. The line is slightly asymmetric and is field dependent. The zero-field extrapolated linewidth δ_0 was measured at room temperature as a function of concentration and is shown in Fig. 2. The homogeneous broadening δ_0 is due to nuclear dipole-dipole interaction. By calculating the Van Vleck second moment due to the dipolar interaction of ^{19}F nuclei of type I_0 with like fluorine nuclei, unlike fluorine nuclei (i.e., of type I_1 and I_2) and ^{55}Mn nuclei one finds for the linewidth (in rad/sec) assuming a Gaussian line shape

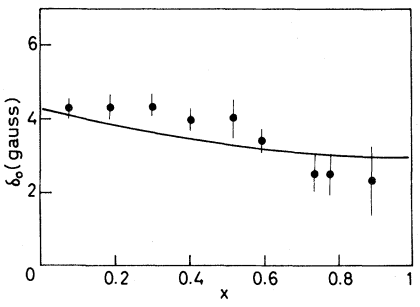

FIG. 2. Room-temperature homogenous linewidth, i.e., extrapolated at zero-external magnetic field of resonance I_0 as a function of concentration in $KMn_xMg_{1-x}F_3$ samples. The line represents the theoretical dipolar linewidth calculated according to Eq. (2).

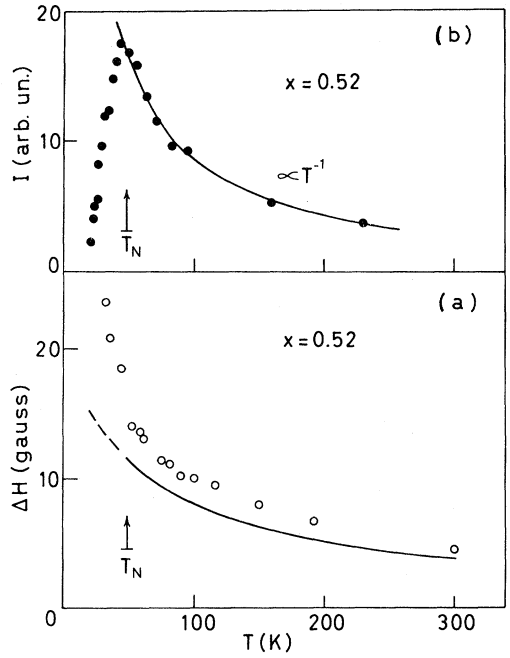

FIG. 3. (a) Linewidth between the points of maximum derivative of signal I_0 in $KMn_xMg_{1-x}F_3$ as a function of temperature at a resonance frequency of 22 MHz. The curve is the theoretical result obtained by using Eqs. (2) and (3) as explained in the text. (b) Intensity of the I_0 line calculated from Eq. (4) plotted as a function of temperature. The curve indicates the behavior expected if all nuclei were to contribute to the observed signal without change of the line shape.

$$\delta_0=2\{\Delta[(1-x)^2+\tfrac{4}{9}(2x-x^2)]+\Delta' x\}^{1/2}, \qquad \Delta=2.9\times10^9,\ \ \Delta'=7.6\times10^7, \tag{2}$$

where Δ and Δ' are in $\sec^{-2}\mathrm{rad}^2$. The comparison of theory and experiments, shown in Fig. 2, can be considered satisfactory.

For the magnetic fields used here, $H\sim5$ kG, a major source of broadening is the inhomogeneity of the local field. Each ^{19}F nucleus of type I_0 is surrounded by a different configuration of second, third, etc., NN Mn^{2+} ions and thus it is subjected to a different local field due to the dipolar interaction with the electronic magnetic moments. A calculation of the variance of the local fields in the paramagnetic phase done by averaging over all spin configurations and orientations of the crystalline domains yields

$$\Delta H=(\langle\Delta H^2\rangle)^{1/2}=\sqrt{P_{||}(x)}\frac{\langle\mu_{||}\rangle}{a^3}=\frac{\sqrt{P_{||}(x)}}{a^3}\left[\frac{C_{\mathrm{at}}}{T+\vartheta(x)}\right]H \tag{3}$$

expressed in G, where C_{at} is the Curie constant per atom and $P_{||}(x)$ is a polynomial in x whose value varies almost linearly from zero at $x=0$ to almost 6 at $x=0.6$ and it remains then practically constant up to $x=1$. When the inhomogenous broadening is relevant the line shape is no longer Gaussian and we can make only a semiquantitative analysis of the data by comparing the measured linewidth with the total variance of the local fields given by the square root of the sum of the second moments due to the nuclear dipolar interaction [Eq. (2)] and the one due to the nuclear-electron dipolar interaction [Eq. (3)]. We find good agreement for the temperature dependence of the linewidth at all concentrations. An example is shown in Fig. 3(a).

When the system becomes antiferromagnetically ordered ($T<T_N$) the inhomogenous broadening should be calculated by considering the random orientation of the local dipolar field. By averaging over all spin configurations of the "flopped" phase and orientations of the crystalline domains one finds that the main contribution to the inhomogenous broadening is given by an expression similar to Eq. (3) with $\langle\mu_{||}\rangle$ replaced by $\mu_{\mathrm{staggered}}$.

However, in this case the major part of the signal moves out into the wings escaping experimental detection. The linewidth measured as the distance between the points of maximum derivative shows only a minor deviation from the behavior in the paramagnetic phase as shown in Fig. 3(a). On the other hand, the normalized intensity of the central part of the signal measured by

$$I=\frac{h(\Delta H)^2}{\Delta H_m}, \tag{4}$$

where h is the peak to peak height of the derivative signal, ΔH is the width between the points of maximum derivative, and ΔH_m is the amplitude of the ac modulation of the magnetic field, drops to a small value starting at T_N as exemplified in Fig. 3(b). The measurements of signal intensity can be used to monitor the ordering temperature T_N. However, the method does not seem to be very practical particularly when the transition is broadened by concentration gradients and one would like to estimate an average transition temperature.

In fact, the disappearence of the signal intensity would be gradual even for a perfectly homogeneous sample due to the nuclei which experience a small local field in the ordered phase because of the spatial symmetry of the surrounding spin configuration. As a matter of fact, these nuclei contribute to a small residual signal which we could detect in the

ordered phase even well below T_N. Thus, we prefer to determine T_N by means of the rf susceptibility method as explained in Sec. IV C.

2. *Spin-lattice relaxation rate*

The nuclear spin-lattice relaxation rate of ^{19}F nuclei of type I_0 as a function of concentration at room temperature was reported previously.[2] It was shown that the relaxation is dominated by the direct dipolar interaction of the ^{19}F nuclei with isolated clusters of Mn ions, namely ions or groups of ions with no Mn NN. The validity of this interpretation was later confirmed in detailed theoretical calculations by Thayamballi and Hone.[4] In another paper we suggested[3] that only the nuclei which are close to an isolated cluster relax by direct interaction while other ^{19}F nuclei of type I_0 further away from the clusters relax by direct interaction with the Mn in the infinitely connected cluster and by spin diffusion to the nuclei next to the isolated clusters. This analysis was largely based on the behavior of the recovery of the nuclear magnetization which displays an initial fast decay accounting for about 20–30% of the signal followed by an almost exponential decay at longer times. The data of T_1 discussed in Refs. 2–4 were obtained by excluding the initial fast recovery. Here, we limit ourselves to report in Fig. 4(a) the temperature dependence of T_1^{-1} measured from the asymptotic behavior at long times of the recovery of the nuclear magnetization. If the relaxation rate is controlled by the nuclear-spin diffusion from the nuclei close to the isolated clusters to the remaining nuclei then one expects that T and H should affect T_1^{-1} mainly through the nuclear-spin diffusion coefficient D. As a first approximation, one may assume[5] $D \propto (\Delta H)^{-1}$ since mutual spin-flip processes which preserve the Zeeman energy are less probable if the resonance frequency is spread over a wide interval: It can be shown[3] that in the "diffusion vanishing" limit $T_1^{-1} \propto D^{1/2}$ and thus $T_1^{-1} \propto (\Delta H)^{-1/2}$. The dependence of the relaxation rate on the linewidth is shown in Fig. 4(b) with the temperature being the implicit parameter. A few measurements with the field H as an implicit parameter are also in qualitative agreement with the above argument. We can conclude that the temperature dependence of the relaxation rate supports the hypothesis that the long-time asymptotic behavior of the recovery is controlled by nuclear-spin diffusion. Under these circumstances a search for a critical-like behavior of T_1^{-1} as $T \rightarrow T_N$ can be done only by carefully separating the different contributions to the nuclear relaxation. We have not attempted this, since single crystals with small concentration gradients should be used for such a study. Preliminary measurements in single crystals of MnF_2:Zn and FeF_2:Zn appear to have been very successful in this respect.[6]

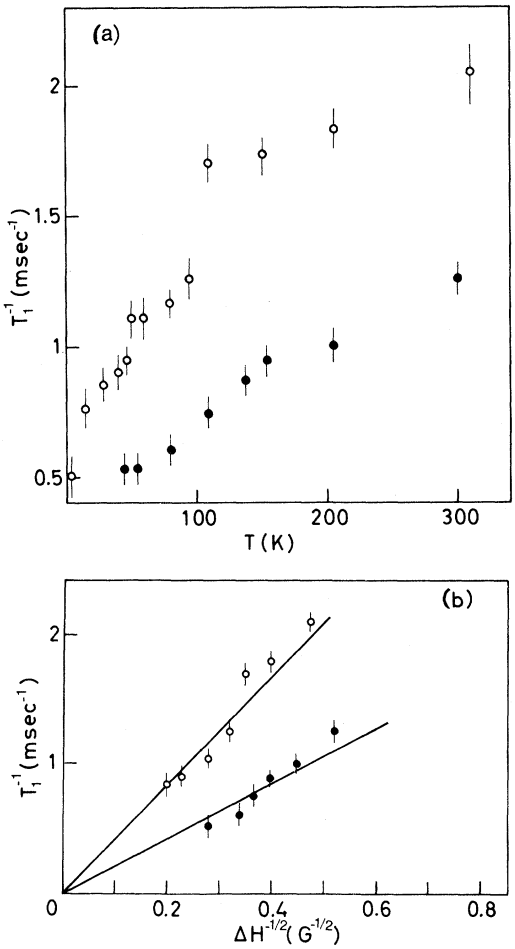

FIG. 4. Relaxation rate as a function of temperature for resonance I_0 in $KMn_xMg_{1-x}F_3$ with (○) $x=0.52$ and (●) $x=0.74$ at the operating frequency of 22 MHz. (a) T_1^{-1} is plotted as a function of temperature. (b) T_1^{-1} is plotted as a function of the inverse square root of the linewidth, the temperature being the implicit parameter.

B. I_1 resonance: Fluorine nuclei with one Mn NN

The resonance I_1 provides, in principle, information about the local magnetic susceptibility, through the measurement of the paramagnetic shift, and about the spectral density of the autocorrelation function, through the linewidth and relaxation measurements.

1. Linewidth and relaxation

As it can be seen in Fig. 1 the resonance I_1 has the asymmetric shape that arises from averaging the orientation of the external field direction, with respect to the axes of the paramagnetic shift tensor, in a powder.[5] The homogeneous width δ_1 was determined by extrapolating at $H=0$ the measurements as a function of the field with the procedure illustrated in Sec. II. The resonance I_1 is dominated by the strong transferred hfs coupling to a single Mn^{2+} ion. Since the hfs field is modulated very fast by the exchange interaction, the measurement of the homogeneous linewidth is equivalent to the measurement of the nuclear spin-lattice relaxation rate,[5] both are a direct probe of the spectral density of the fluctuations at small frequencies (at $\omega=0$ and $\omega_L \simeq 0$). The results at room temperature as a function of concentration were reported previously.[2] The large enhancement of the linewidth with increasing magnetic dilution has been attributed to the enhancement at low frequency of the spectral density of the autocorrelation function.[2,3] In fact, by reducing the manganese concentration the effective dimensionality of the magnetic exchange path decreases from $d=3$ towards $d\simeq 1$ near the percolation threshold. Correspondingly, there is a slowing down of the decay at long times of the autocorrelation function since this goes as $t^{-d/2}$ for the diffusive behavior typical of an Heisenberg system.

In Fig. 5 the temperature dependence of the homogenous linewidth for samples having different concentrations is reported. The linewidth increases drastically as the ordering temperature is approached and it becomes too large to be measured at about 10–20 K from the ordering temperature preventing us from investigating the nonclassical critical region. The broadening of the line reflects the slowing down of the fluctuations of the electronic magnetic moments due to the buildup of the antiferromagnetic correlation. It is compared in the next section with the predictions of the RMFA theory.

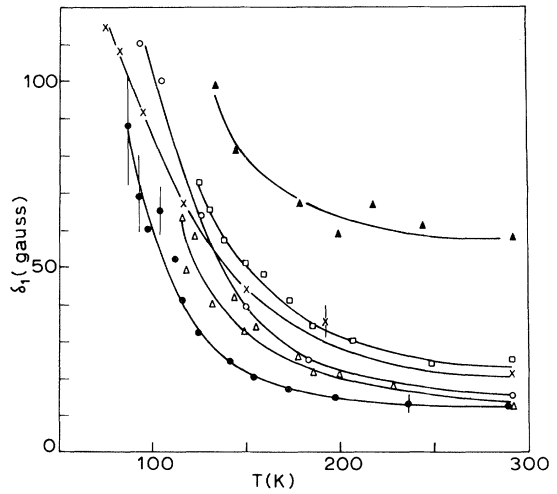

FIG. 5. Zero-field extrapolated linewidth of resonance I_1 plotted as a function of temperature in $KMn_xMg_{1-x}F_3$ for different concentrations: (●) $x=0.89$; (△) $x=0.78$; (○) $x=0.6$; (×) $x=0.52$; (□) $x=0.41$; (▲) $x=0.305$. The curves are a guide to the eye.

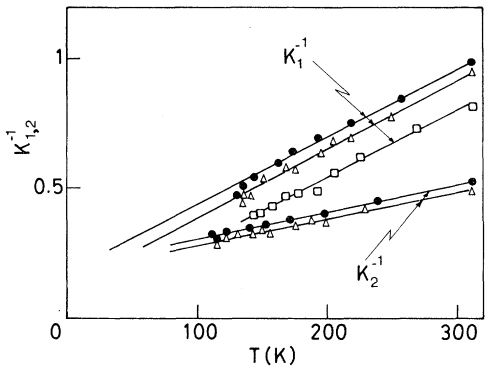

FIG. 6. Inverse of the paramagnetic shift in percent plotted as a function of temperature for $KMn_xMg_{1-x}F_3$ with (●) $x=0.89$; (△) $x=0.74$, and (□) $x=0.41$. The subscripts 1 and 2 refer to line I_1 and I_2, respectively. The straight lines indicate the Curie-Weiss behavior.

2. Paramagnetic shift

The paramagnetic shift of the ^{19}F nucleus in pure $KMnF_3$ single crystal is anisotropic due to the nuclear-electron dipolar interaction. In the $KMn_xMg_{1-x}F_3$ polycrystalline samples the line shape is asymmetric as expected from averaging the anisotropic shift over the crystal orientations and over the configurations of magnetic ions second NN to the given ^{19}F nucleus. The problem of measuring the isotropic part of the paramagnetic shift is then similar to the one encountered in metal powders displaying anisotropic Knight shift.[7] The measured isotropic shift $K_1=(\Delta H/H)100$ is shown in Fig. 6 as a function of temperature for some values of the concentration. The shift can be fitted with a Curie-Weiss law $\propto (T+\vartheta)^{-1}$ but the value of ϑ is different from the one obtained from measurements of uniform susceptibility[8] and from measurements of the shift of line I_2 (see next paragraph). This is not surprising since the shift of line I_1 is proportional to the local thermal average of the magnetic moment of the Mn^{2+} ions NN to a ^{19}F of type I_1, i.e., $K_1 \propto \langle \mu \rangle$ but for a disordered system, lacking translational invariance, $\langle \mu \rangle$ is not necessarily the

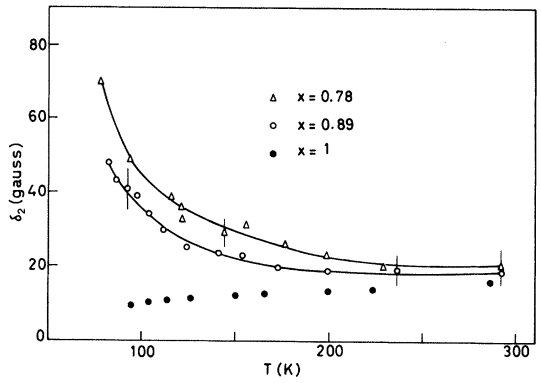

FIG. 7. Zero-field extrapolated linewidth of resonance I_2 plotted as a function of temperature. The data (●) referring to pure $KMnF_3$ are from Ref. 9. The curves are a guide to the eye.

same for every Mn^{2+} ion. This point is clarified in the next section where the shifts of lines I_1 and I_2 are compared.

C. I_2 resonance: Fluorine nuclei with two Mn NN

The measurements of the I_2 resonance were performed only in the two samples of higher Mn concentration since the I_2 line intensity drops off very rapidly by increasing the magnetic dilution (see Fig. 1).

1. Linewidth and relaxation

The results for the homogenous linewidth as a function of temperature are shown in Fig. 7. The broadening observed as the ordering temperature is approached can be contrasted with the line narrowing observed in pure $KMnF_3$.[9] Since the ^{19}F nucleus of type I_2 has both the Mn^{2+} ions NN one would have expected to see a line narrowing as in pure $KMnF_3$. The narrowing in pure $KMnF_3$ is associated with the cancellation of the contribution to the NMR linewidth due to the electron-spin autocorrelation terms by the pair-correlation ones, this cancellation being exact for the antiferromagnetic mode which dominates the spectral density as $T \to T_N$. The divergence observed here must be associated with the lack of translational invariance for the disordered systems. A more quantitative discussion is postponed to the next section.

2. Paramagnetic shift

The paramagnetic shift $K_2 = (\Delta H/H)100$ of line I_2 measured in the same way as for the line I_1 is shown in Fig. 6 as a function of temperature. In this case the temperature dependence can be fitted with a Curie-Weiss behavior with "apparent" Curie-Weiss temperatures which are larger than the one obtained from the shift of line I_1 in the same sample. This indicates that the Curie-Weiss plot cannot be used to analyze these measurements of local susceptibility. In fact, the average molecular field seen by the Mn^{2+} ions NN to the fluorine nuclei of type I_1 is different from the one seen by the ions next to I_2. A comparison of the local susceptibilities in terms of the RMFA is discussed in the following section.

IV. DISCUSSION OF THE EXPERIMENTAL RESULTS

The measurements of paramagnetic shift and of line broadening for the resonances I_1 and I_2 contain information about the correlation and fluctuations of the Mn^{2+} magnetic moments as the ordering temperature is approached. In the following we compare the experimental results with the theoretical predictions based on RMFA.

A. Comparison of the paramagnetic shifts of line I_1 and I_2

The isotropic part of the paramagnetic shift of the ^{19}F nuclei can be written as[1]

$$K_n = \frac{\Delta H}{H} = \frac{nA\langle S\rangle}{\gamma_N \hbar H} = \frac{nA\chi_{\rm at}}{\gamma_N g \mu_B \hbar} , \tag{5}$$

where μ_B is the Bohr magnetron and $g=2$ for the Mn^{2+} ion, γ_N is the nuclear gyromagnetic ratio, and $\chi_{\rm at}$ is the susceptibility per manganese atom; the transferred hyperfine interaction constant A is multiplied by the number n of Mn NN to the given ^{19}F nucleus on the assumption that the local hyperfine field is additive.

The local susceptibilities for the Mn^{2+} ions next to fluorine nuclei of type I_1 and I_2, respectively, can be expressed in terms of a simple RMFA picture as[10]

$$\chi^1_{\rm at} = \chi_{\rm at}\left[1+\frac{x\vartheta_N}{zT}\right] ,$$
$$\chi^2_{\rm at} = \chi_{\rm at}\left[1+\frac{x\vartheta_N}{zT}\left[1-\frac{1}{x}\right]\right] , \tag{6}$$

where ϑ_N is the Curie temperature of pure $KMnF_3$, $z=6$ is the magnetic NN coordination number for

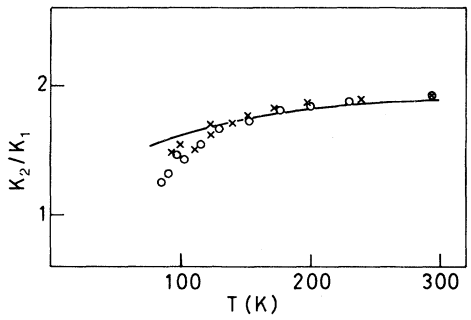

FIG. 8. Ratio of the paramagnetic shifts of line I_2 and I_1 plotted as a function of temperature. The curve is the theoretical behavior of $2\chi^2_{at}/\chi^1_{at}$ from Eq. (6).

the Mn atom, and $\chi_{at}=(C_{at}/T+x\vartheta_N)$ is the uniform susceptibility per manganese atom.

By using $J=3.8$ K one has $\vartheta_N=2zJS(S+1)/3k_B=133$ K and by using $\mu_{eff}=g\mu_B[S(S+1)]^{1/2}$ for the effective Mn^{2+} magnetic moment one finds for the atomic Curie constant $C_{at}=7.3\times10^{-24}$ cm^3 K yielding a susceptibility in good agreement with the experimental results.[11]

First we test the RMFA and the hypothesis that the coupling constant A is additive by comparing the temperature dependence of the ratio K_2/K_1 with the quantity $2\chi^2_{at}/\chi^1_{at}$ from Eqs. (6).

As can be seen in Fig. 8 the agreement is reasonable except for temperature below ~120 K, where the RMFA is likely to be insufficient to describe the local effects associated with the different environment of Mn atoms next to fluorine of types 1 and 2, respectively.

Before comparing the concentration dependence of the paramagnetic shifts with the theory we have to take into account the temperature and concentration dependence of the hfs constant A and of the exchange interaction J. By using the high-temperature results by Dormann *et al.*[12] one has approximately

$$\frac{1}{A}\frac{\partial A}{\partial T}\sim-1.5\times10^{-4}\ \mathrm{K}^{-1}$$

and

$$\frac{1}{J}\frac{\partial J}{\partial T}\sim-2.4\times10^{-4}\ \mathrm{K}^{-1}\ .$$

These temperature dependences lead to corrections which are well within our experimental error for the temperature interval investigated. The concentration dependence can be estimated by assuming[13,14]

$$\left.\frac{\partial \ln J}{\partial \ln R}\right|_{R=R_0}=-10$$

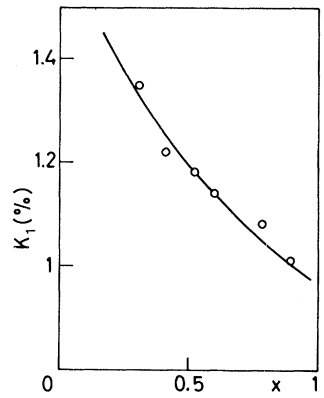

FIG. 9. Paramagnetic shift of line I_1 plotted as a function of concentration for samples of $KMn_xMg_{1-x}F_3$ at room temperature. The curve is the theoretical prediction according to Eq. (8) with the hfs interaction constant A as an adjustable parameter.

for small variations of the interionic distance around the value R_0. Also, since the ^{19}F hfs interaction is proportional to the Mn^{2+}-F^- overlap integrals and the Mn^{2+}-F^-Mn^{2+} superexchange interaction is proportional to the square of these integrals one may expect[12] $J\propto A^2$ and thus

$$\left.\frac{\partial \ln A}{\partial \ln R}\right|_{R=R_0}=-5\ .$$

By using the concentration dependence of the lattice parameter given in Sec. II, i.e.,

$$\frac{1}{a}\frac{\partial a}{\partial x}=5\times10^{-2}$$

one can write approximately

$$\begin{aligned} J(x)&=J[1+0.5(1-x)]\ ,\\ A(x)&=A[1+0.25(1-x)]\ . \end{aligned} \tag{7}$$

The concentration dependence of J in Eq. (7) agrees closely with the one estimated in Ref. 8.

Finally, the expression for the percent shift of line I_1 is

$$K_1=\frac{A\,100[1+0.25(1-x)]C_{at}}{\gamma_N g\mu_B\hbar\{T+x\vartheta_N[1+0.5(1-x)]\}}\times\left[1+\frac{x\vartheta_N[1+0.5(1-x)]}{zT}\right]. \tag{8}$$

The experimental results for the concentration dependence of K_1 are compared with the theory [Eq. (8)] in Fig. 9. The theory fits the experiments for $A=(13.3\pm0.5)\times10^{-4}$ cm^{-1} quite well. This value is somewhat lower than the value obtained for pure $KMnF_3$, i.e., $A=(16.26\pm0.4)\times10^{-4}$ cm^{-1}.

The difference may very well arise from the change of the Mn^{2+}-F^- overlap integral due to the substitution of the adjacent Mn^{2+} ion with a Mg^{2+} ion.

In conclusion the RMFA theory gives a satisfactory description of the static NMR results. The concentration dependence of the hfs constant and of the exchange interaction are well described by considering the average change in lattice spacing and the local effects associated with the Mg substitution.

B. Temperature dependence of the I_1 and I_2 linewidths

The basic theory describing the temperature dependence of the relaxation rates and linewidths in a dense paramagnetic insulator was given by Moriya years ago[15] and later reformulated by Sherer *et al.*[9] so as to include the effects of short-range order.

The ^{19}F NMR homogenous linewidth due to the transferred hfs interaction with the NN Mn^{2+} ions can be written

$$\delta = K_B T \hbar^{-2} N^{-1} \sum_{\vec{q}} \frac{|A(\vec{q})|^2 \chi(\vec{q})}{\Gamma_{\vec{q}}} , \tag{9}$$

where the q-dependent coupling constant is given by

$$|A(\vec{q})|^2 = \begin{cases} 2A^2(1+\cos q_x a) & \text{for line } I_2 \\ A^2 & \text{for line } I_1 , \end{cases} \tag{10}$$

with x in the $Mn^{2+}-F^--Mn^{2+}$ bond direction. The generalized susceptibility expressed so as to include the Onsager reaction field is

$$\chi(\vec{q}) = \frac{\chi_0 T / T_N^0}{s - J(\vec{q})/J(\vec{k}_0)} , \tag{11}$$

where $\chi_0 = S(S+1)/k_B T$, $\vec{k}_0$ is the antiferromagnetic critical wave vector and

$$s = [1 + \chi_0 \lambda(T)] \frac{T}{T_N^0} \tag{12}$$

is a parameter related to $\lambda(T)$, the Onsager correction to the MFA. The simplest adaptation of this theory to the case of a randomly diluted paramagnet is done by rescaling the above expressions in terms of the RMFA transition temperature

$$T_N^0 = \frac{2xzJ(x)S(S+1)}{3k_B}$$

$$= 133x[1 + 0.5(1-x)] \tag{13}$$

expressed in K, where we used Eq. (7) and the value $J = 3.8$ K pertaining to $KMnF_3$.

Regarding the relaxation rate Γ_q for the collective spin-correlation function one can use the expression used by Moriya[15] and modified with the Onsager correction,[9] namely

$$\Gamma_q = \pi^{1/2} \tau \hbar^{-2} J(k_0) k_B T \left[s - \frac{J(q)}{J(k_0)} \right] \times \left[1 - \frac{J(q)}{J(0)} \right] \left[\frac{s T_N^0}{T} - 1 \right] . \tag{14}$$

The final expressions for the linewidths normalized to the infinite temperature value are

$$\frac{\delta_2}{\delta_\infty} = \frac{2[G(1)+G(s)](1+s)^{-2} + (s-1)G'(s)(1+s)^{-1}}{6[sG(s)-1][2G(1)-1]} \tag{15}$$

for the line I_2 and

$$\frac{\delta_1}{\delta_\infty} = \frac{[G(1)+G(s)](1+s)^{-2} - G'(s)(1+s)^{-1}}{6G(1)[sG(s)-1]} \tag{16}$$

for the line I_1, where

$$G(s) = (2\pi)^{-3} \int_{-\pi}^{\pi} d^3q \left[s + \tfrac{1}{3}(\cos q_x + \cos q_y + \cos q_z) \right]^{-1} ,$$

$$G'(s) = \frac{\partial G(s)}{\partial s} .$$

Equation (15) is identical to the one given in Refs. 9 and 16 for the cases of pure $KMnF_3$ and pure $RbMnF_3$.

Equations (15) and (16) predict for the linewidths of lines I_2 and I_1 the universal behaviors shown in Fig. 10 which is in complete disagreement with the experimental results. This fact proves that a theory relying on the translational invariance of the mag-

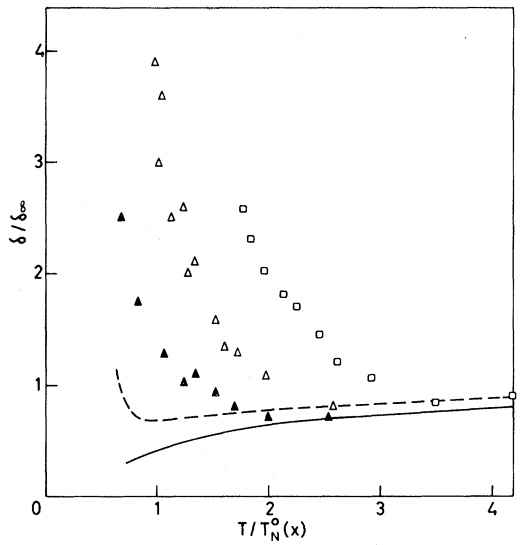

FIG. 10. Normalized homogenous linewidth plotted as a function of the normalized temperature in $KMn_xMg_{1-x}F_3$: (▲) δ_2 for $x=0.78$; (△) δ_1 for $x=0.78$; (□) δ_1 for $x=0.41$. The full line represents the theoretical prediction of Eq. (15) while the dashed line the one of Eq. (16).

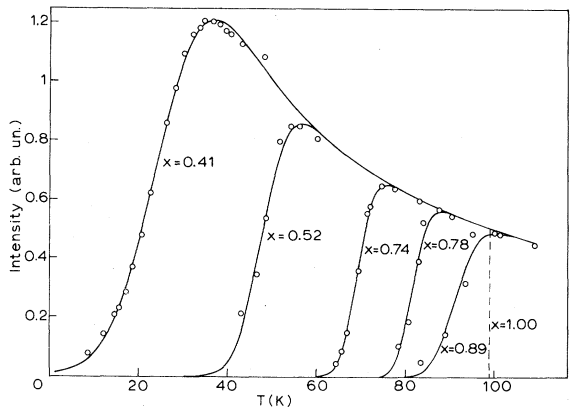

FIG. 11. Intensity of the modulated rf signal at 22 MHz in zero-external magnetic field plotted as a function of temperature in $KMn_xMg_{1-x}F_3$ for the different concentrations indicated in the figure. The curves represent the best fit obtained by assuming that the intensity drops to zero for $T<T_N$ and that a Gaussian distribution of transition temperatures is present in the mixed samples. (The analytical expression is $I \propto (1/T) \times \mathrm{erf}[\sqrt{2}(T-T_N)/\Delta T_N]$.

netic lattice to treat collective effects in the wave-vector space is completely inappropriate in this case and that a theory treating the local variables in real space should be used instead.

Here, we limit ourselves to some qualitative comments. The presence of a divergent linewidth for line I_2 indicates that the cancellation of the critical antiferromagnetic fluctuations at $q=K_0=\pi/a$ by the coupling constant $|A(q)|$ [see Eq. (10)] is ineffective. In other words, the strength of the critical fluctuations appears to be different at different Mn^{2+} sites. The same kind of local effects may be responsible for the behavior of line I_1 which seems to diverge much more strongly than expected (see Fig. 10). It should also be noted that, due to experimental uncertainty, the measured linewidth may also include a static inhomogeneous component due to the increasing, as the temperature decreases, of the distribution of the local isotropic paramagnetic shifts even though this contribution should have been in principle eliminated by the procedure of extrapolating the width at zero external magnetic field. Again, measurements in single crystals are needed to distinguish with certainty among the different sources of line broadening.

C. Concentration dependence of the transition temperature

The value of the ordering temperature in a site-diluted antiferromagnet can be determined in several ways. The methods that have been used in $KMnF_3$:Mg are discontinuity in the temperature derivative of the uniform susceptibility,[8] ^{19}F NMR,[8] and broadening of the EPR line.[17] These methods suffer from limitations in the precision with which T_N can be determined unless single crystals with no concentration gradients are utilized.[18] The measurements of the temperature derivative of the linear birefringence has proved to be a powerful method in noncubic systems like MnF_2:Zn and Fe:Zn.[19] The application of this method to $KMnF_3$:Mg is complicated by the fact that the system is nearly cubic and that it displays structural phase transitions in the temperature region of interest. We chose here to use the method[20] based on the measurement of the intensity of the EPR signal in zero-external magnetic field as described in Sec. II. As long as the system is paramagnetic one observes a maximum of rf susceptibility at $H\simeq 0$. When the system becomes antiferromagnetically ordered the resonance in the ac susceptibility shifts to the microwave region. As a consequence, the signal intensity at the operating frequency of 22 MHz drops to zero as shown in Fig. 11. The disappearance of the signal is very abrupt in pure $KMnF_3$ while it occurs over a range of a few degrees in the mixed crystals. The broadening of the transition region is most likely due to the concentration gradients across our samples since these are in the form of large chunks (~ 1 g) of polycrystalline material obtained by slow cooling from the melt. Since the

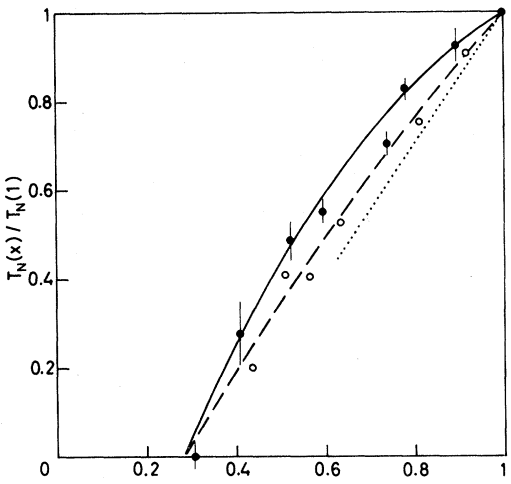

FIG. 12. Normalized average transition temperature vs Mn concentration in $KMn_xMg_{1-x}F_3$. (●) present work; (○) Ref. 8. The curves are theoretical predictions as explained in the text. The error bars represent the width of the transition region as obtained from the best-fit procedure on the data of Fig. 11.

concentration determined by x-ray is an average concentration it seems appropriate to relate it to the average value of the transition temperature. Thus, the intensity versus temperature curves in Fig. 11 have been fitted assuming a Gaussian distribution of transition temperatures centered at T_N and having a width ΔT_N. The values of T_N obtained from a best-fit procedure are plotted in Fig. 12 as a function of magnetic concentration where the "error bar" represents the width of the transition as obtained from the best fit. The fact that the width of the transition increases drastically as the percolation concentration is approached, and therefore $\partial T_N(x)/\partial x$ increases, is in qualitative agreement with the assumption that the broadening is associated with concentration gradients in the samples. It should be noted that for a 3D site-diluted Heisenberg system in which the critical epxonent of the specific heat $\alpha < 0$, the phase transition is expected to be perfectly sharp.[21]

The concentration dependence of T_N is compared in Fig. 12 with the theoretical predictions. The dashed curve is the result of recent calculations based on real-space renormalization techniques for $S = \frac{1}{2}$ Heisenberg systems[22,23] and the dotted line represents the result of a coherent-potential approximation calculation for a simple cubic lattice with predominantly first NN interaction.[24] Both the above theoretical curves assume a NN exchange interaction which does not change upon dilution. If we modify the dashed curve by allowing for the concentration dependence of the exchange interaction as approximated by Eq. (7) we obtain the full curve which is in better agreement with our experimental results. It should be noted that the previous measurements by Breed *et al.*[8] seem to agree more with the curve which does not include the correction for the concentration dependence of J. The data by Breed *et al.* may be affected by a systematic error due to the neglect of the concentration gradients in the analysis of the data.

ACKNOWLEDGMENTS

We are very grateful to Professor V. Jaccarino who has provided the samples and who has stimulated this work with pertinent suggestions and criticisms. We would like to thank Dr. G. Rossi for the x-ray analysis of the samples and Professor R. G. Barnes for the hospitality offered in his laboratory where part of this work was performed. Ames Laboratory is operated for the U. S. Department of Energy by Iowa State University under Contract No. W-7405-Eng-82. This research was supported by the Director for Energy Research, Office of Basic Energy Sciences, WPAS-KC-02-02-02.

[1]R. G. Shulman and K. Knox, Phys. Rev. 119, 94 (1961).

[2]F. Borsa and V. Jaccarino, Solid State Commun. 19, 1229 (1976).

[3]G. D'Ariano, R. L. Lecander, C. Marchetti, and F. Borsa, J. Magn. Magn. Mater. 15, 681 (1980).

[4]P. Thayamballi and D. Hone, Phys. Rev. B 21, 1766 (1980).

[5]A. Abragam, *The Principles of Nuclear Magnetism* (Oxford University Press, Clarendon, 1961).

[6]H. Yasuoka, S. P. Vernon, and V. Jaccarino (unpublished).

[7]F. Borsa and R. G. Barnes, J. Phys. Chem. Solids 25, 1305 (1964).

[8]D. J. Breed, K. Gilijamse, J. W. Sterkenburg, and A. R. Miedema, J. Appl. Phys. 41, 1267 (1970); Physica (Utrecht) 68, 303 (1973).

[9]C. Scherer, J. E. Gulley, D. Hone, and V. Jaccarino, Rev. Bras. Fis. 4, 299 (1974).

[10]J. E. Gulley and V. Jaccarino, *17th Conference on Magnetism and Magnetic Materials, Chicago, 1971,* edited by C. D. Graham, Jr. and J. J. Rhyne, (AIP, New York, 1972), p. 403.

[11]K. Hirakawa, H. Hirakawa, and T. Hashimoto, J.

Phys. Soc. Jpn. 15, 2063 (1960).
[12]E. Dormann, D. Hone, and V. Jaccarino, Phys. Rev. B 14, 2715 (1976).
[13]D. Bloch, J. Phys. Chem. Solids 27, 881 (1966).
[14]K. C. Johnson and A. J. Sievers, Phys. Rev. B 10, 1027 (1974).
[15]T. Moriya, Progr. Theor. Phys. 16, 23 (1956); 16, 641 (1956); 28, 371 (1962).
[16]L. L. Hess and E. R. Hunt, Phys. Rev. B 6, 45 (1972).
[17]R. P. Gupta, M. S. Seehra, and W. E. Vehse, Phys. Rev. B 5, 92 (1972).
[18]R. A. Dunlap and A. M. Gottlieb, Phys. Rev. B 23, 6106 (1981).
[19]D. P. Belanger, F. Borsa, A. R. King, and V. Jaccarino, J. Magn. Magn. Mater. 15, 807 (1980).
[20]V. Jaccarino (private communication).
[21]A. Brooks Harris, J. Phys. C 7, 1671 (1974).
[22]R. B. Stinchcombe, J. Phys. C 12, 4533 (1979).
[23]D. Kumar, R. B. Pandey, and M. Barma, Phys. Rev. B 23, 2269 (1981).
[24]R. A. Tahir-Kheli and A. R. McGurn, J. Phys. C 11, 1413 (1978).